RESEARCH ARTICLE | MARCH 26 2012

Reversibility of the zinc-blende to rock-salt phase transition in cadmium sulfide nanocrystals

R. Martín-Rodríguez; J. González; R. Valiente; ... et. al

Journal of Applied Physics 111, 063516 (2012)
https://doi.org/10.1063/1.3697562

Reversibility of the zinc-blende to rock-salt phase transition in cadmium sulfide nanocrystals

R. Martín-Rodríguez,[1] J. González,[2,a)] R. Valiente,[1] F. Aguado,[2] D. Santamaría-Pérez,[3] and F. Rodríguez[2]
[1]*MALTA Consolider-Team, Dpto. Física Aplicada, Facultad de Ciencias, Universidad de Cantabria, Avda. de Los Castros s/n, 39005 Santander, Spain*
[2]*MALTA Consolider-Team, Dpto. CITIMAC, Facultad de Ciencias, Universidad de Cantabria, Avda. de Los Castros s/n, 39005 Santander, Spain*
[3]*MALTA Consolider-Team, Dpto. Química Física I, Facultad de Ciencias Químicas Universidad Complutense de Madrid, Avda. Complutense s/n, 28040 Madrid, Spain*

(Received 10 November 2011; accepted 20 February 2012; published online 26 March 2012)

CdS nanoparticles prepared by a mechanochemical reaction in a planetary ball mill have been investigated by x-ray diffraction, optical absorption, and Raman scattering under high pressure conditions up to 11 GPa. The zinc-blende (ZB) to rock-salt phase transition is observed around 6 GPa in all experiments, the transition pressure being similar to the one measured in CdS colloidal nanocrystals, and much higher than in bulk (around 3 GPa). The direct optical energy gap in ZB-CdS increases with pressure, and suddenly drops when the pressure is raised above 6 GPa, according to the high-pressure indirect-gap behavior. A linear blue-shift of the CdS Raman spectra is observed upon increasing pressure. Both Raman and x-ray diffraction studies indicate that the phase transition has a large hysteresis, making the ZB phase barely recoverable at ambient conditions. Cell parameters and bulk modulus measured in CdS nanoparticles clearly show that the nanoparticles at ambient conditions are subject to an initial pressure in comparison to CdS bulk.
 [http://dx.doi.org/10.1063/1.3697562]

I. INTRODUCTION

The interest in semiconductors, which can be spatially confined to a few tens of nanometers, has increased in last decades. Interdisciplinary studies from bioimaging to materials science, including LEDS or solar technology, have extended the relevance of these nanomaterials. Their physical properties can be quite different from those of the bulk and, hence, an ample field involving new materials conformations and physico-chemical phenomena has appeared. For instance, there are many works showing a decrease in the melting temperature[1–3] as well as an increase of the transition pressure[4,5] with decreasing nanoparticle size. The relatively high surface energy in nanoparticles may account for this behavior, making their high-pressure phase less stable than in bulk.[4] Besides, nanoparticles probably lack the internal defects, which act as nucleation points for structural phase transitions in bulk.[6] Three dimensionally confined electron-hole systems, known as quantum dots, have unusual optical properties that may lead to novel applications in opto-electronics.[7] Strong exciton confinement effects are expected when the crystal size is lower than the exciton effective Bohr radius.[8] For instance, the effective bandgap in CdSe can be tuned from deep red (1.7 eV) to green (2.4 eV) by reducing the nanocrystal diameter from 50 to 2 nm,[9] and in CdS it varies from green (2.47 eV) to deep blue (4 eV) by reducing the particle size from 30 to 2 nm.[10] Phonon confinement also occurs when the particle size is small enough to consider the phonon described by a wave packet rather than a plane wave.[11] Both the softening and the asymmetric broadening at the low energy side of the Raman peaks are in good agreement with an effective relaxation of the q-vector selection rule due to quantum size effects.

CdS is a well-studied II-VI direct gap semiconductor due to its many applications.[9,12] The bulk crystallizes in the hexagonal wurtzite (W) structure, while both W and cubic zinc-blende (ZB) structures have been found in CdS nanoparticles.[13] High-pressure spectroscopy is a very useful tool to understand the electronic structure of semiconductors, as well as to detect phase transformations. Bulk CdS undergoes a W to rock-salt (RS) phase transition at 2.7 GPa.[14–18] It is a first-order reconstructive transition with a 19% volume decrease, and a change in coordination number of both Cd and S from 4 to 6. In this work, we have performed x-ray diffraction (XRD), optical absorption, and Raman measurements at high pressure in order to characterize the ZB to RS phase transition in CdS nanoparticles prepared by ball milling. Interestingly, surface modes are easily detected in CdS nanoparticles by Raman measurements due to the high surface to volume ratio. Regarding structural properties, we are also interested in elucidating whether transformation from bulk to nanoparticle involves a change of density and/or crystal structure, as it may affect phase stability and physical properties of CdS.

II. EXPERIMENTAL SECTION

CdS nanocrystals showing an intense orange color were prepared in a planetary ball mill.[19] The starting materials

a)Author to whom correspondence should be addressed. Electronic mail: jesusantonio.gonzalez@unican.es.

$CdCl_2$, Na_2S, and NaCl were grinded in a Retsch PM 400/2 under high-purity argon atmosphere at 300 rpm, using hardened steel vials and balls and a ball-to-powder mass ratio of 20:1. NaCl, used as a diluent to prevent nanoparticles aggregation, was removed with distilled water. XRD patterns at ambient pressure (AP) were recorded using the Cu-Kα radiation ($\lambda = 1.5418$ Å) of a 1700 diffractometer (Philips). High pressure XRD experiments were carried out with a Xcalibur diffractometer (Oxford Diffraction Limited) using Mo-Kα source ($\lambda = 0.7107$ Å) and a 135 mm Atlas CCD detector placed at a distance of 90 mm from the sample. This setup has been proved to be suitable for obtaining structural information on similar compounds (including nanostructured ones) under high pressure in recent works.[20,21] The indexing and refinement of the powder patterns were carried out using the TOPAS package (Bruker AXS 2005, V3). Transmission electron microscopy (TEM) was performed on a JEM 2100 electron microscope (JEOL, Japan). The samples were prepared by suspending the solid powder in ethanol (Panreac, 96% purity) under ultrasonic vibration. One drop of the prepared suspension was applied to carbon films on copper (Agar Scientific).

The experimental set-up used for room temperature (RT) optical absorption measurements has been described elsewhere.[22] The T64000 Raman spectrometer system (Horiba) together with the 514.5 nm green line of an Innova Spectrum 70 C Kripton-Argon laser (Coherent) and a Nitrogen-cooled CCD (Jobin-Yvon *Symphony*) with a confocal microscope for the detection were employed in Raman experiments. High pressure measurements were performed in gasketed diamond anvil cells. A membrane cell was utilized for optical measurements while XRD experiments were performed in a modified Merrill-Bassett type cell (MALTA design).[23] Paraffin and silicone oil (Dow Corning 200 fluid)[24] were used as pressure transmitting media in spectroscopic (Raman and optical absorption) and XRD studies, respectively. In any case experiments were performed within their hydrostatic ranges.

III. RESULTS AND DISCUSSION

A. Synthesis and characterization

Depending on the particle size, different structures have been identified for CdS nanocrystals. (i) When the size is smaller than 5 nm, CdS nanoparticles mainly crystallize in the metastable cubic ZB structure (space group *F4-3 m*). (ii) When the size is larger than about 8 nm, they are stable in the hexagonal W structure ($P6_3mc$). (iii) In between, they adopt intermediate phases.[13] In both ZB and W structures, each anion is surrounded by four cations at the corners of a tetrahedron and vice versa. The small energy difference for the two phases explains the observed polymorphism at ambient conditions.[25]

Figure 1 shows the XRD pattern (Cu-Kα) of CdS nanoparticles together with a Rietveld refinement using both W and ZB phases. The composition of the sample can be roughly estimated through the performed structural refinement. However, due to the phase coexistence and the probable puzzling structural disposition, also found in similar nanostructured compounds,[26] the uncertainty in the percentage of each phase is pretty large. In any case, the best fitting (Fig. 1) corresponds to a 85% ZB-15% W mixed structure. Different sets of constraints led to an important dispersion in this variable, showing a minimum contribution of 65% from the ZB phase. The cell parameter of the ZB phase, $a = 5.78$ Å, is slightly but significantly smaller than in bulk, $a_0 = 5.818$ Å.[27] The values for the W structure, $a = 4.11$ Å and $c = 6.58$ Å, are somewhat different to those of the bulk ($a_0 = 4.137$ Å and $c_0 = 6.7144$ Å).[28] The $c/a = 1.60$ ratio in nanoparticles deviates 1% from that of the bulk ($c_0/a_0 = 1.62$); this estimation of the W structure distortion is smaller than the up to 15% difference observed by Kumpf *et al.*[26] Nevertheless, the present results point out that there is a volume contraction (density increase) on passing from bulk to nanoparticle in both ZB and W phases.

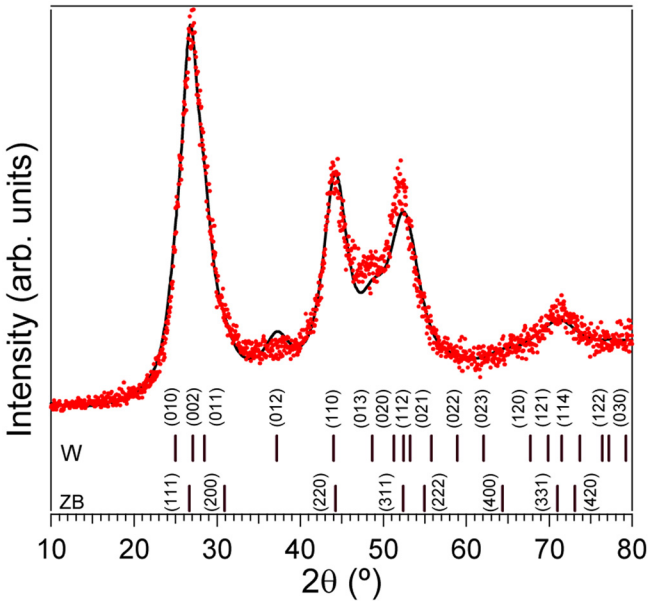

FIG. 1. XRD pattern of the CdS nanocrystalline samples prepared by ball milling. The line corresponds to the calculated pattern for the 85% ZB-15% W mixed structure, and vertical ticks indicate the (hkl) index for each crystallographic phase.

The average size of the nanoparticles is 5 nm as derived from the Bragg peak broadening according to the Williamson-Hall equation.[29] This model includes not only the size effect (through the Scherrer equation) but also the strains. The obtained value is in good agreement with the TEM results shown in Fig. 2. However, TEM images also show that the samples consist of particles of different shapes and sizes; from spherical nanoparticles of about 5 nm in size to bigger particles and nanorods of about 3–5 nm in width.

B. X-ray diffraction under pressure

Figure 3 shows the evolution of the XRD patterns of CdS nanoparticles under high pressure up to 7.5 GPa in both up-stroke and down-stroke runs. It is observed that low pressures stabilize the ZB-CdS structure (W-CdS phase is not detectable in any pattern) and related peaks shift to higher Bragg angles with increasing pressure, which is consistent with a uniform volume reduction. However, this phase starts to transform into the RS structure at 4.3 GPa, and both

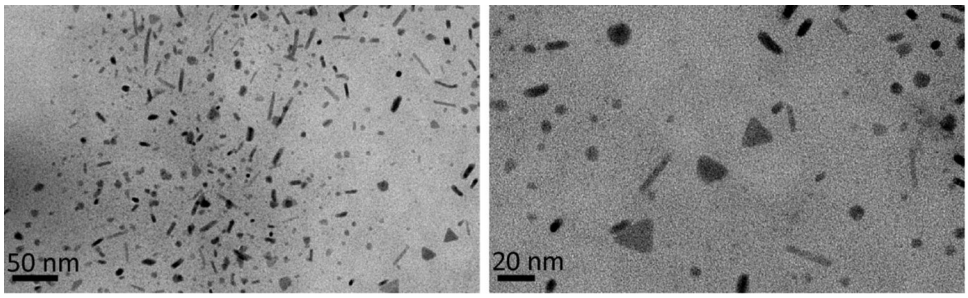

FIG. 2. TEM images of CdS nanocrystals prepared by ball milling.

phases coexist between 4.3 and 5.4 GPa. Above this pressure, only the RS structure is observed. Preceding XRD studies showed that bulk W-CdS crystals transformed to the RS structure between 2 and 3 GPa.[17,18] In our experiments, the RS phase remains upon pressure release and no trace of ZB phase has been detected in the high pressure regime (downstroke). Due to the limited access to the reciprocal space and the particular character of the nanostructured sample, the cell parameters at different pressures were determined by the Pawley method, restricting the number of free variables. Either ZB or RS phases were considered before and after the phase transition, respectively, while both structures were used for the fittings in the pressure range of phase coexistence (4.3–5.4 GPa).

The volume dependence on pressure is shown in Fig. 4. It can be observed that volume reduces by 7% from 0 to 5 GPa, whereas it abruptly decreases by 15%, from 186 to 154 Å^3, at the phase transition. Bulk moduli for both phases were determined using a Murnaghan's equation of state[30] with first derivative fixed ($B_0' = 4$). From these data we conclude that the ZB ($B_0 = 74 \pm 2$ GPa) is more compressible than the RS $B_0 = 107 \pm 5$ GPa. Furthermore, the bulk modulus for ZB-CdS single crystals is about 64 GPa,[31] and ca. 85 GPa for RS-CdS single crystals.[18,32] This result clearly indicates that CdS nanoparticles are less compressible than CdS bulk, consistently with nanoparticle densification, as it is confirmed by the reduction of cell parameters on passing from nanoparticles to bulk. An increase in both the relative volume change at the transition pressure, and the bulk modulus when decreasing particle size was also found in Ag and Au nanoparticles,[33] as well as in some oxides, like Fe_2O_3.[34] However this effect, which has been ascribed to surface effects, should not be considered a general trend in nanoparticle since an opposite behavior was observed in other oxides.[21] The competition between surface and bulk effects can lead to opposite behaviors depending on the size, shape and structure of the nanoparticle. Investigations along this line are needed in order to clarify this subtle fact.

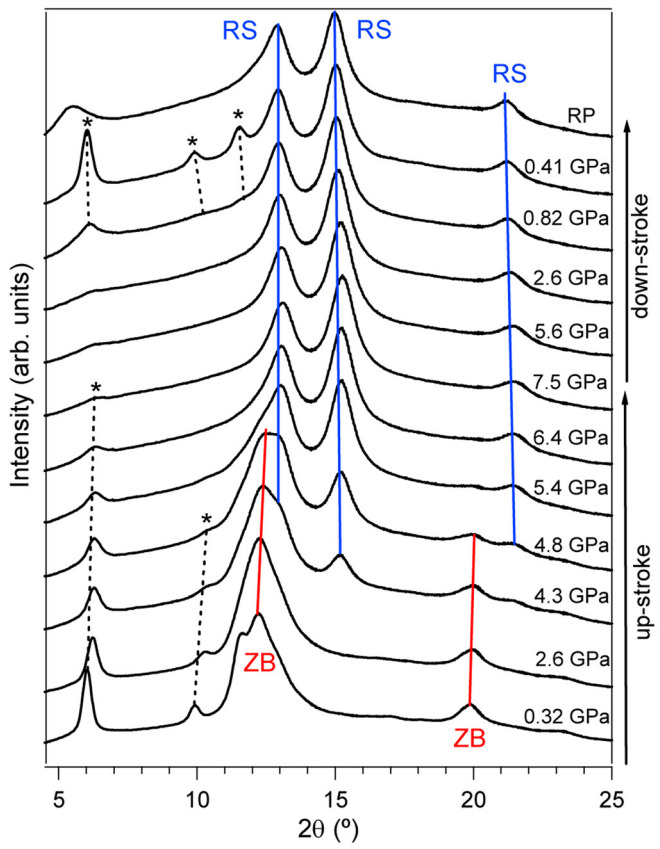

FIG. 3. XRD patterns of CdS nanoparticles under high pressure. Asterisks represent the diffraction peaks of the pressure transmitting medium (silicone oil).

C. Absorption under pressure

In W-CdS bulk, the $\Gamma_{15}^V \rightarrow \Gamma_1^C$ direct gap corresponds to the lowest energy transition ($E_g = 2.4$ eV at 300 K) whereas indirect gaps occur at least 1 eV above E_g and always lie above E_g at high pressure.[35] *Ab-initio* calculations of the

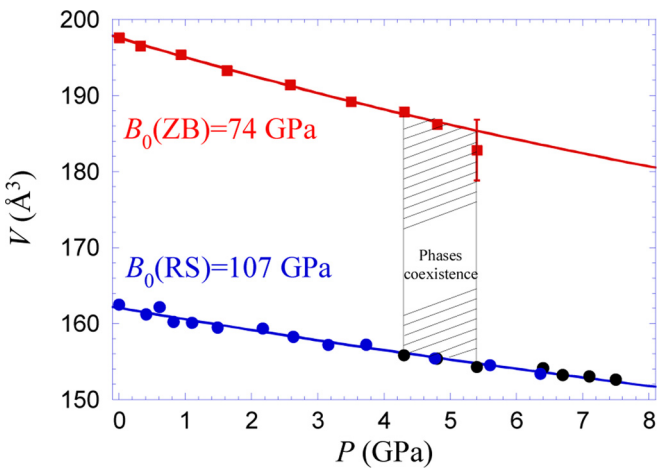

FIG. 4. Isothermal equation of state of CdS nanoparticles for the ZB (red squares) and RS (black circles in the up-stroke and blue circles in the down-stroke) structures. Errors are smaller than symbol size; otherwise bars are explicitly depicted. In both cases the volume dependence on pressure has been fitted to a Murnaghan equation of state with $B_0' = 4$.

electronic structure in W- and ZB-CdS showed that the fundamental direct bandgap in both structures differs by less than 0.1 eV.[36] Since the exciton Bohr radius in CdS bulk is 2.6 nm,[37] CdS nanocrystals with the metastable ZB structure (diameter around 5 nm) are in the weak confinement regime. Therefore, the direct optical energy gap of bulk and nanocrystals ought to be similar. Some representative absorption spectra of CdS nanocrystals at different pressures are shown in Fig. 5.

The analysis of spectra at low pressures indicates that the absorption at the fundamental edge can be described by a direct gap transition law,

$$\alpha(\hbar\omega) = A\left(\hbar\omega - E_g\right)^{\frac{1}{2}}. \quad (1)$$

This result is in agreement with the band structure of the metastable ZB structure of CdS at AP.[35,36] When the pressure is raised above 6 GPa, the CdS nanocrystals suddenly become brown colored, and a large and abrupt red-shift in the absorption edge is observed. Previous high-pressure optical studies in bulk CdS indicated an abrupt red-shift in the optical absorption edge at 2.7–3.0 GPa, and this was interpreted as a result of the first-order W-to-RS phase transition.[14,15] Moreover, the ZB-to-RS transition was observed at 8 GPa in CdS colloidal nanocrystals.[38] In this work, the ZB-to-RS phase transition is also detected at pressures much higher than the bulk transition pressure of ca. 3 GPa. This behavior has been usually observed in nanocrystalline semiconductors of the group IV as well as III-V or II-VI in comparison to the bulk counterpart.[39] The high transition pressure can be explained by the larger surface tension of the RS-phase nanocrystals compared to ZB-CdS.[6] An example of the absorption edge for the high pressure RS phase recorded at 6.1 GPa is shown in Fig. 5. It must be noted that

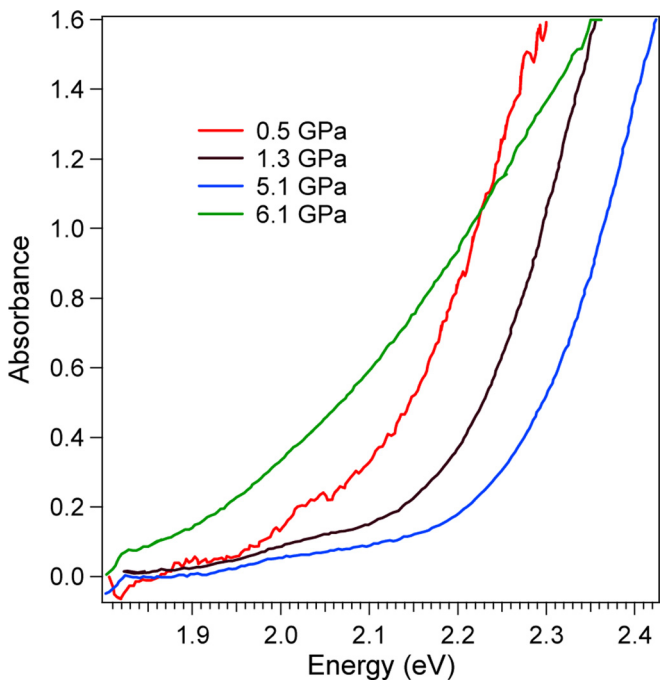

FIG. 5. Below bandgap shift from the RT absorption spectra of CdS nanoparticles with hydrostatic pressure.

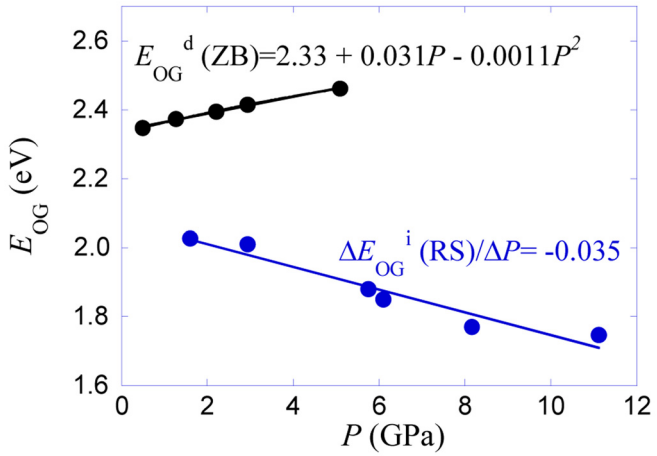

FIG. 6. Pressure dependence of the optical bandgap energy, E_{OG}, in both ZB and RS structures for CdS nanocrystals.

the RS-phase edge is strikingly different compared to the ZB-phase edge in CdS nanocrystals, what is a clear indication of an indirect gap transition.

The ZB-CdS optical bandgap energy, E^d_{OG}(ZB), has been obtained by extrapolating the α^2 versus $\hbar\omega$ fitting curves to $\alpha = 0$. The resulting blue-shifted E^d_{OG}(ZB) pressure dependence is shown in Fig. 6. Measurements of semiconductor energy gaps under hydrostatic pressure are worth for band-structure determination in tetrahedrally bonded semiconductors. As indicated elsewhere,[40,41] in a given compound series, equivalent energy band extremals have similar pressure coefficients, which are positive for direct Γ_v-Γ_c transitions, but they can vary widely among nonequivalent extremals, being negative for indirect Γ_v-X_c. For most semiconductors, the variation of the direct bandgap with pressure can be described by a quadratic expression[38]

$$E_{OG}(P) = E_{OG}(0) + aP + bP^2. \quad (2)$$

The fit of the experimental data to Eq. (2) gives: $E_{OG}(0) = 2.33$ eV, $a = 31 \pm 4$ meV/GPa, and $b = -1.1 \pm 0.3$ meV/GPa.[2] The obtained linear coefficient is smaller than the one reported for the direct gap energy for ZB-CdS colloidal nanoparticles, 45.7 meV/GPa,[33] and for bulk W-CdS, 45.5 ± 0.5 meV/GPa.[15] In Fig. 6, the estimated indirect gap energy in the RS phase, E^i_{OG}(RS), is also plotted as a function of pressure. E^i_{OG}(RS) values have been obtained by extrapolating the linear $\alpha^{1/2}$ versus $\hbar\omega$ plots to $\alpha = 0$. The fitted linear pressure coefficient is -35 ± 5 meV/GPa. A similar negative shift was observed in II-VI analog semiconductors in the RS phase at high pressure.[35] Theoretical predictions on the band structure of RS semiconductors at high pressure show that RS-CdS is an indirect gap semiconductor. At variance with ZB-CdS, the valence band maximum shifts with pressure from the Γ point toward the L and K points as a result of p-d hybridization. The conduction band minimum X_c is below the Γ_c minimum, with two types of indirect gap, namely L_v-X_c and Σ_v-X_c, which have negative pressure coefficients.[15] Nevertheless, the indirect bandgap of CdS nanoparticles in the high pressure RS phase is difficult to determine due to the formation of band-tail states, probably caused by defects created throughout the phase transition. The highest

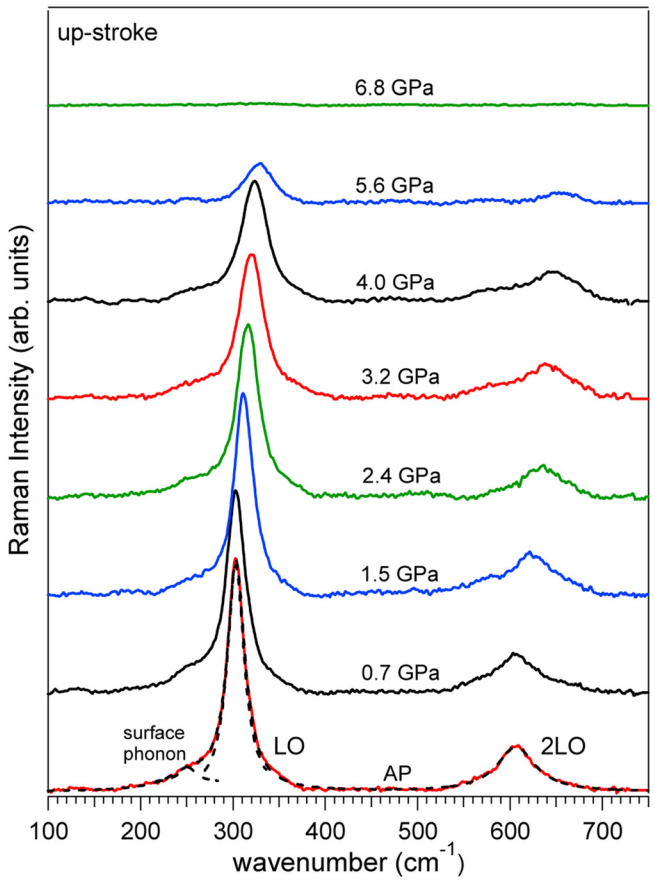

FIG. 7. RT Raman spectra of CdS nanoparticles at different pressures (up-stroke).

pressure achieved in the up-stroke run was 11 GPa. Absorption spectra have also been recorded upon releasing pressure down to 1.6 GPa. As observed in Fig. 6, the bandgap does not revert to its original value in the ZB phase within this pressure range. This behavior is clearly opposite to the reversible sharp transition with no hysteresis observed in CdS colloidal nanocrystals by Haase and Alivisatos.[38]

D. Raman spectroscopy at high pressure

The Raman spectra of CdS nanoparticles have been studied at RT under hydrostatic pressure up to 7 GPa (Fig. 7). The phonon frequencies were obtained by fitting the experimental peaks to Lorentzian functions, and the fitting curve at ambient conditions is also presented in Fig. 7. Table I reports the Raman peak position, ω_i, and full width at half maximum, $\Delta\omega_i$, of the fitted Lorentzians.

TABLE I. Frequency, ω, and width, $\Delta\omega$, of surface, LO and 2LO phonon modes at ambient conditions derived from the Raman spectra.

Assignment	ω_i/cm^{-1}	$\Delta\omega_i/\text{cm}^{-1}$	$(\text{d}\omega/\text{d}P)/\text{cm}^{-1}/\text{GPa}$
Surface	254.1	27.5	1.4
LO	303.4	11.6	4.8
2LO	606.4	25.3	9.2

The longitudinal optical (LO and 2LO) modes shift linearly with pressure to higher energies at a rate of 4.8 ± 0.2 cm^{-1}/GPa for LO, and 9.2 ± 0.4 cm^{-1}/GPa for 2LO (Fig. 8(a)). These values are in good agreement with previous results for bulk W-CdS[16,42] and ZB-CdS colloidal nanocrystals.[38] As observed the intensity of the Raman phonons (LO, 2LO) gradually decreases with pressure. In a Stokes process, the Raman intensity within a single two-band model, depends in first approximation on $1/(E_g\text{-}E_l)$,[43] where E_g is the bandgap and E_l is the energy of the laser incident photons. At AP, the direct energy gap of ZB-CdS nanoparticles are very close to the laser photon energy (~2.4 eV), but E_g increases with pressure at a rate of 0.031 eV GPa^{-1}. Under pressure, the Raman peak intensity decreases due to the increase of $(E_g\text{-}E_l)$ from nearly zero at AP to 0.155 eV at 5 GPa.

The frequency change observed at AP in CdS nanocrystals with respect to bulk is noteworthy. It can be understood considering two opposite effects. Firstly, the LO mode shifts around 1.6 cm^{-1} to lower energy when nanoparticle size is reduced to 5 nm, as a consequence of the quantum confinement.[44] Secondly, the cell parameter contraction observed in nanoparticles produces an effective pressure of about 1.0 GPa on the nanoparticle. This internal pressure induces an effective energy shift of 4.8 cm^{-1}, according to the LO pressure coefficient, 4.8 ± 0.2 cm^{-1}/GPa. Both effects yield a slight but neat blueshift of the phonon mode of 3.2 cm^{-1} on passing from bulk to nanoparticle. It must be noted that, although both effects partially compensate the opposite Raman shifts, there is a neat mode hardening that confirm the densification processes attained in CdS nanoparticles.

The Grüneisen parameter (γ_i) for a quasi-harmonic mode i of frequency ω_i is defined by

$$\gamma_i = -\frac{d\ \text{In}\ \omega_i}{d\ \text{In}\ V} = \frac{1}{\beta}\frac{\partial\ \text{In}\ \omega_i}{\partial P} = \frac{B_0}{\omega_i}\frac{d\omega_i}{dP}, \qquad (3)$$

where B_0 is the bulk modulus of CdS nanoparticles (74 GPa, see above), β is the isothermal volume compressibility, and

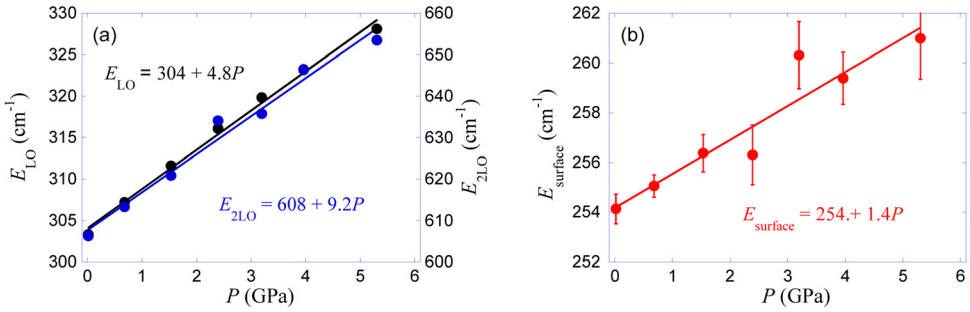

FIG. 8. Pressure dependence of the energy of the observed phonons, E_{ph}, for CdS nanocrystals. LO and 2LO Raman modes (a), and surface mode (b).

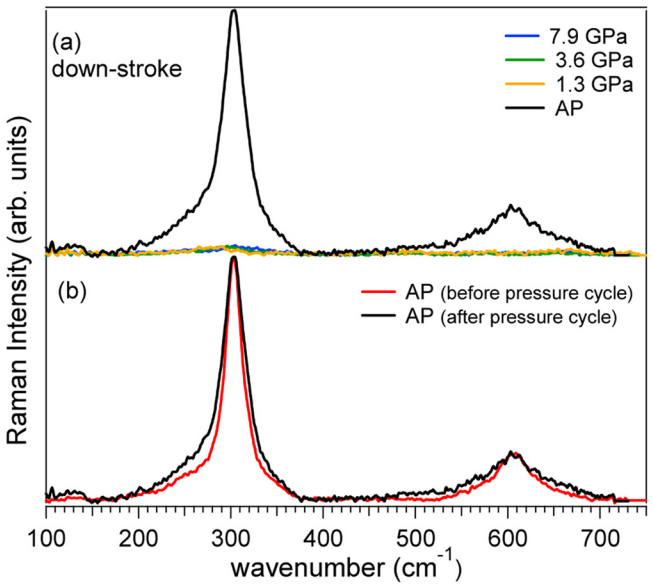

FIG. 9. RT Raman spectra of CdS nanoparticles upon decreasing pressure (a) and comparison between the AP Raman spectra before and after the pressure cycle (b).

V is the molar volume. The obtained Grüneisen parameter for the LO mode is, $\gamma_{LO} = 1.13$. This value is similar to the Grüneisen parameters of the polar phonons in tetrahedral semiconductors.[45] In addition to the first-order LO and the overtone 2LO modes, a shoulder ascribed to a surface mode is observed in the low energy side of the LO mode.[46] In nanocrystals, the contribution of the surface scattering may be comparable to Raman scattering from the volume; the surface to volume atomic ratio is about 7% for CdS nanoparticles with 5 nm in size. Scott and Damen also reported the observation of surface modes in CdS by Raman spectroscopy.[47] The dependence of the surface mode energy on pressure is shown in Fig. 8(b).

Above 6.8 GPa the Raman peaks disappear proving the ZB-to-RS phase transition in CdS nanocrystals. As expected from symmetry considerations, the RS phase should not have associated first-order Raman active phonons. The Raman spectra of the CdS nanocrystals have been recorded after the phase transition by decreasing pressure from 8 GPa to AP. The data, which are shown in Fig. 9(a), indicate that no Raman peak is recovered down to 1.3 GPa and, therefore, the RS phase remains within this pressure range. Nevertheless, LO and 2LO Raman modes appear again when pressure is released to AP. We conclude that the ZB-to-RS phase transition is reversible although presents a large hysteresis of about 5 GPa. Figure 9(b) compares the Raman spectra of CdS nanoparticles at AP before and after the phase transition. The fact that both spectra are centered at the same frequency indicates that no appreciable change in size is induced by the phase transition.

IV. CONCLUSIONS

We demonstrate that CdS nanocrystals prepared in a planetary ball mill crystallize in the metastable ZB cubic structure with an average size of 5 nm. The ZB-to-RS phase transition has been detected by three different techniques: XRD, optical absorption and Raman spectroscopy. From XRD measurements under high pressure we show that ZB-CdS nanoparticles undergo a transition into the RS structure above 5.4 GPa, with bulk modulus of $B_0 = 74 \pm 2$ GPa and $B_0 = 107 \pm 5$ GPa for the low-pressure and high-pressure structures, respectively. The comparison of V_0 and B_0 obtained in CdS bulk and nanoparticles clearly indicates that there is a density increase in the nanoparticles, which become less compressible. These variations have been associated with surface effects. The direct gap energy of ZB-CdS nanoparticles increases with pressure at a rate of $\alpha = 31 \pm 4$ meV/GPa, transforming to an indirect gap above 6 GPa, with its energy changing with pressure at a rate of -35 ± 5 meV/GPa. The energy of LO and 2LO Raman modes for CdS nanoparticles increases with pressure at a similar rate as W-CdS bulk. Raman measurements evidence that the ZB-to-RS phase transition for CdS nanocrystals takes place at around 6 GPa, as well as the recovery of the ZB structure at AP. The reversibility of the phase transition was not found by XRD, probably due to the residual stress on the sample after pressure release. The stability domain of the ZB structure increases up to 6 GPa at RT for 5 nm-size CdS nanocrystals as it has been demonstrated through three independent experiments. Finally, both XRD and Raman measurements as a function of pressure are consistent with the increase of density upon CdS bulk transformation into nanoparticles.

ACKNOWLEDGMENTS

This work was financially supported by the Spanish Ministerio de Ciencia e Innovación (Projects MAT2008-06873-C02-01/MAT, MAT2011-28868-C02-01 and CTQ2009-14596-C02-01), the Comunidad de Madrid and European Social Fund (Project S2009/PPQ-1551 4161893 (QUIMAPRES)), and the MALTA-Consolider Ingenio 2010 (Reference CSD2007-00045). R.M.-R. thanks the Spanish MEC for a FPI research grant (Reference BES-2006-13359). The expert assistance of L. Rodríguez at the SERTEM is gratefully acknowledged.

[1]Q. Jiang, C. C. Yang, and J. C. Li, Mater. Lett. **56**, 1019 (2002).
[2]S. Xiao, W. Hu, and J. Yang, J. Phys. Chem. B **109**, 20339 (2005).
[3]S. H. Tolbert and A. P. Alivisatos, Annu. Rev. Phys. Chem. **46**, 595425 (1995).
[4]S. M. Clark, S. G. Prilliman, C. K. Erdonmez, and A. P. Alivisatos, Nanotech. **16**, 2813 (2005).
[5]S. M. Tolbert and A. P. Alivisatos, Science **265**, 373 (1994).
[6]K. Jacobs, D. Zaziski, E. C. Scher, A. B. Herhold, and A. P. Alivisatos, Science **293**, 1803 (2001).
[7]A. P. Alivisatos, Science **271**, 933 (1996).
[8]L. E. Brus, J. Chem. Phys. **90**, 2555 (1986).
[9]M. Bruchez, Jr., M. Moronne, P. Gin, S. Weiss, and A. P. Alivisatos, Science **281**, 2013 (1998).
[10]L. E. Brus, J. Chem. Phys. **80**, 4403 (1984).
[11]H. Richter, Z. P. Wang, and L. Levy, Solid State Commun. **39**, 625 (1981).
[12]A. H. Mueller, M. A. Petruska, M. Achermann, D. J. Werder, E. A. Akhadov, D. D. Koleske, M. A. Hoffbauer, and V. I. Klimov, Nano Lett. **5**, 1039 (2005).
[13]C. Ricolleau, L. Audinet, M. Gandais, and T. Gacoin, Eur. Phys. J. D **9**, 565 (1999).
[14]A. L. Edwards and H. G. Drickamer, Phys. Rev. **122**, 1149 (1961).
[15]B. Batlogg, A. Jayaraman, J. E. Van Cleve, and R. G. Maines, Phys. Rev. B **27**, 3920 (1983).

[16]U. Venkateswaran, M. Chandrasekhar, and H. R. Chandrasekhar, Phys. Rev. B **30**, 3316 (1984).
[17]N. B. Owen, P. L. Smith, J. E. Martin, and A. J. Wright, J. Phys. Chem. Solids **24**, 1519 (1963).
[18]H. Sowa, Solid State Sci. **7**, 73 (2005).
[19]R. Martín-Rodríguez, R. Valiente, F. Rodríguez, and J. González, High Press. Res. **29**, 482 (2009).
[20]D. Santamaria-Perez, A. Vegas, C. Muehle, and M. Jansen, Acta Cryst. **B67**, 109 (2011).
[21]D. Errandonea, D. Santamaria-Perez, V. Grover, S. N. Achary, and A. K. Tyagi, J. Appl. Phys. **108**, 073518 (2010).
[22]B. Amaya Moral and F. Rodríguez, Rev. Sci. Instrum. **66**, 5178 (1995).
[23]E. del Corro, M. Taravillo, J. González, and V. G. Baonza, Carbon **49**, 973 (2011).
[24]D. D. Ragan, D. R. Clarke, and D. Schiferl, Rev. Sci. Instrum. **67**, 494 (1996).
[25]A. Mujica, A. Rubio, A. Muñoz, and R. J. Needs, Rev. Mod. Phys. **75**, 863 (2003).
[26]C. Kumpf, R. B. Neder, F. Niederdraenk, P. Luczak, A. Stahl, M. Scheuermann, S. Joshi, S. K. Kulkarni, C. Barglik-Chory, C. Heske, and E. Umbach, J. Chem. Phys. **123**, 224707 (2005).
[27]R. W. G. Wyckoff, *Crystal Structures* (Wiley, New York, 1963), Vol. 2.
[28]Y. N. Xu and W. Y. Ching, Phys. Rev. B **48**, 4335 (1993).
[29]G. K. Williamson and W. H. Hall, Acta Metall. **1**, 22 (1953).
[30]F. D. Murnaghan, P. Natl. Acad. Sci. **30**, 244 (1944).
[31]F. Bechstedt and W. A. Harrison, Phys. Rev. B **39**, 5041 (1989).
[32]T. Suzuki, T. Yagi, S. Akimoto, T. Kawamura, S. Toyoda, and S. Endo, J. Appl. Phys. **54**, 748 (1983).
[33]J. Z. Jiang, J. S. Olsen, L. Gerward, and S. Morup, Europhys. Lett. **44**, 620 (1998).
[34]Q. F. Gu, G. Krauss, W. Steurer, F. Gramm, and A. Cervellino, Phys. Rev. Lett. **100**, 045502 (2008).
[35]M. Cardona and G. Harbeke, Phys. Rev. **137**, A1467 (1965).
[36]K. J. Chang, S. Froyen, and M. L. Cohen, Phys. Rev. B **28**, 4736 (1983).
[37]H. S. Nalwa, *Handbook of Nanostructured Materials and Nanotechnology* (Academic, New York, 2000).
[38]M. Haase and A. P. Alivisatos, J. Phys. Chem. **96**, 6756 (1992).
[39]A. San-Miguel, Chem. Soc. Rev. **35**, 876 (2006).
[40]W. Paul, J. Phys. Chem. Solids **8**, 196 (1958).
[41]J. Gonzalez, F. V. Perez, E. Moya, and J. C. Chervin, J. Phys. Chem. Solids **56**, 335 (1995).
[42]C. A. Arguello, D. L. Rousseau, and S. P. S. Porto, Phys. Rev. **181**, 1351 (1969).
[43]P. Y. Yu and B. Welter, Solid State Commun. **25**, 209 (1978).
[44]J. González, J. Marquina, F. Rodríguez, and R. Valiente, High Press. Res. **29**, 594 (2009).
[45]J. M. Besson, J. P. Itié, A. Polian, G. Weill, J. L. Mansot, and J. Gonzalez, Phys. Rev. B **44**, 4214 (1991).
[46]M. Abdulkbadar and B. Thomas, Nanostruct. Mater. **5**, 289 (1995).
[47]J. F. Scott and T. C. Damen, Optics Communications **5**, 410 (1972).